Hindawi Publishing Corporation
Journal of Nanomaterials
Volume 2010, Article ID 186486, 11 pages
doi:10.1155/2010/186486

Research Article

Stable Aqueous Suspension and Self-Assembly of Graphite Nanoplatelets Coated with Various Polyelectrolytes

Jue Lu,[1,2] Inhwan Do,[1] Hiroyuki Fukushima,[1] Ilsoon Lee,[2] and Lawrence T. Drzal[1]

[1] *Composite Materials and Structures Center, Michigan State University, East Lansing, MI 48824-1226, USA*
[2] *Department of Chemical Engineering and Materials Science, Michigan State University, East Lansing, MI 48824-1226, USA*

Correspondence should be addressed to Ilsoon Lee, leeil@msu.edu and Lawrence T. Drzal, drzal@egr.msu.edu

Received 1 March 2010; Accepted 7 May 2010

Academic Editor: Rakesh Joshi

Exfoliated graphite nanoplatelets (xGnPs) with an average thickness of 1–10 nm present an inexpensive alternative to carbon nanotubes in many applications. In this paper, stable aqueous suspension of xGnP was achieved by noncovalent functionalization of xGnP with polyelectrolytes. The surfactants and polyelectrolytes were compared with respect to their ability to suspend graphite nanoplatelets. The surface charge of the nanoplatelets was characterized with zeta potential measurements, and the bonding strength of the polymer chains to the surface of xGnP was characterized with Raman spectroscopy. This robust method opens up the possibility of using this inexpensive nanomaterial in many applications, including electrochemical devices, and leads to simple processing techniques such as layer-by-layer deposition. Therefore, the formation of xGnP conductive coatings using layer-by-layer deposition was also demonstrated.

1. Introduction

Considerable interest has been drawn in the layer-by-layer (LbL) self-assembly of nanosized carbon particles due to their excellent thermal, electrical, and mechanical properties [1]. Carbon nanotubes (CNTs) and fullerenes (also known as buckyball or C_{60}) have been intensively studied, and their possible applications in nanodevices [2, 3], quantum wires [4], ultrahigh-strength engineering fibers [5], sensors [6, 7], and support of electrocatalysts [4] are developing. Both carbon nanotubes and fullerenes are expensive, which hinders their application in industry. Recently, the two-dimensional carbon graphene has attracted great attention, due to its exceptionally high crystal and electronic quality [8, 9]. Growth of large area of high-quality graphene was developed on metal substrates [10], and individual graphene sheets can be also prepared by micromechanical cleavage [8]. Unfortunately, these approaches are technically complex and difficult for mass production. In addition, these two-dimensional crystals cannot theoretically exist in the free state [8]. The most commonly used nano sized form of graphene is graphite nanoplatelets, which are a few layers of graphene sheets stacked together and are produced by the exfoliation of graphite via an acid intercalation, followed by ultrasonic irradiation to isolated graphite nanosheets [11]. Research in our group at MSU has led to a process that can successfully produce exfoliated graphite nanoplatelets ($xGnP^{TM}$), which are 1–10 nm in thickness and from 100 to 1000 nm in diameter. The surface of the graphite nanoplatelets is pure graphene where the carbon is in a sp^2 configuration. This presents a uniformly homogeneous and moderately energetic surface that has been shown to be an excellent nucleating surface for both polar and nonpolar polymers. Furthermore, these graphite nanoplatelets possess the high electric conductivity of graphene. With an expected cost on the order of $5/pound, these nanoplatelets could be a suitable substitute for carbon nanotubes and fullerenes for most applications. So far, graphite nanoplatelets are most commonly used in composite application due to their good mechanical properties and electrical conductivity [12–14]. Recently, we have demonstrated that xGnP can be an inexpensive alternative to carbon nanotubes and carbon black as an advantageous support for fuel cell applications, which has the highest thermal-oxidation resistance and the highest degree of graphitization [15]. In addition, xGnP and xGnP-supported electrocatalysts have shown significant catalytic effect toward hydrogen peroxide, resulting highly sensitive and quickly responding glucose biosensors [16, 17].

The major challenge for these hydrophobic carbon nanostructures is their dispersion in an aqueous medium. Several approaches have been studied for the production of aqueous suspension of carbon nanotubes. Chemical modification of the graphene surface is common, such as acid treatment, which imparts –COOH groups at the broken links or at the ends of nanotubes [18, 19]. However, such chemical modification can disrupt the electronic conjugation in carbon nanotubes which inevitably deteriorate the electrical properties of the nanotubes. Another common method is to suspend carbon nanotubes in various surfactants or charged polymers accompanied by the physical processes, which involves high-shear homogenization and ultrasonication [20]. This method became universal for carbon nanotube dispersion because it is easy to control, and most importantly, it preserves the integrity of carbon nanotubes. The functionalized carbon nanotubes are used to construct thin films for various applications.

Since Decher's pioneering work in 1997 [21], the LbL assembly method has been well studied to create highly tuned, functional thin films with nanometer-level thickness [1]. In LbL assembly, oppositely charged polymers are alternately adsorbed on the surface by the electrostatic force, although possible hydrogen bonding, hydrophobic interaction, and van der Waals interactions could also be used. Considerable work has been done on self-assembly of carbon nanotubes. This approach can solve the dispersion problems of carbon nanotubes in polymer matrix, one of the big challenges of the traditional composite processing method. In addition, LbL assembly was also used to incorporate carbon nanotubes in the construction of chemical sensors and biosensors, due to their high electrocatalytic effect, fast electron transfer, rate and large working surface area [22]. Several groups have reported the preparation of self-assembled carbon films using graphite oxide nanoplatelets [23–26]. However, the oxidation of graphite reduced the original conductivity of graphite. To restore the conductivity of the carbon films, the graphite oxide needs to be reduced to the original state by either chemical or electrochemical methods, which is not cost effective. In addition, this additional process may inhibit their use in biosensor application due to the enzyme stability during the reduction process.

In this paper, we report the achievement of stable aqueous dispersions of graphite nanoplatelets and their self-assembly. Since graphite nanoplatelets are not stable in aqueous solution due to the hydrophobic characteristics of graphene sheets and their significant hydrophobic interactions which form agglomerates in aqueous solution. Much effort has been devoted to achieve a stable suspension of graphite nanoplatelets with various surfactants and polyelectrolytes (PEs). In addition, by modifying the charge of polyelectrolytes on the graphite sheet, the agglomeration of graphite nanoplatelets can be possibly prevented by electrostatic or strong repulsive forces due to the surface charge induced by the polyelectrolytes during the self-assembly process. The morphologies of the graphite monolayer and multilayer films have been characterized by the optical microscopy (OM), scanning electron microscopy (SEM) and atomic force microscopy (AFM). Additionally, the resistance and transmittance of these films were also measured.

2. Experimental Procedures

2.1. Materials. Poly(diallyldimethylammonium chloride) (PDAC), sulfated poly(styrene) (SPS), and branched poly ethyleimine (PEI) were purchased from Aldrich. The weight average molecular weights (M_w) of PDAC, SPS, and PEI were ~100,000–200,000, 70,000, and 750,000, respectively. Polyacrylic acid (PAA) (M_w = 90,000) was purchased from Polysciences Inc. Poly(3,4-ethylenedioxythiophene) poly(styrene sulfonate) (PEDT/SPS) (Baytron P V407) was received as a sample from Bayer Corp. and used as received. The surfactants, sodium dodecylbenzene sulfonate (SDBS) and sodium dodecyl sulfate (SDS) were purchased from Aldrich and used as received. Microscope glass slides were purchased from Corning. All aqueous solutions in the processes were prepared using deionized (DI) water (>18.1 MΩ) supplied by a Barnstead Nanopur Diamond-UV purification unit equipped with a UV source and final 0.2 μm filter. All procedures were done at room temperature.

2.2. Preparation of Polyelectrolyte and Surfactant Solutions. Aqueous polyelectrolyte solutions were prepared containing either 20 mM PDAC or 10 mM SPS in 0.1 M NaCl. PEI and PAA solution was prepared containing 0.1 wt% polymer in DI water, and the pH value of the solution was not adjusted. The solutions were filtered with 0.22 μm cellulose acetate membrane filter system from Corning to remove particulates. Other solutions with surfactants (SDBS and SDS) were prepared containing 0.1 wt% surfactants in DI water.

2.3. Preparation of Graphite Suspension. 0.1 g of xGnP was dispersed in 100 mL polyelectrolyte solution by sonication with an output power of 23 W for 30 minutes. The suspension was stirred for 24 hours. The excess polyelectrolyte was removed by filtering through 0.2 μm membrane followed by DI water washing for three times. The polyelectrolyte-coated xGnP was redispersed to 100 mL DI water by mild sonication (output power: 10 W) for 10–15 minutes. The pH value of the suspension with PEI-coated xGnP was adjusted to be between 5.0–6.0.

2.4. Layer-by-Layer Self-Assembly Procedure. To prepare xGnP/polyelectrolyte multilayers, anionic PEs-xGnP such as SPS-xGnP were alternately assembled with PDAC, and cationic PEs-xGnP, such as PEI-xGnP with SPS. First, the glass slides were cleaned twice in an ultrasonic unit, first with a commercially available detergent (Alconox, Alconox Inc.) for 20 minutes and then without for 10 minutes. Slides were dried under a N_2 gas stream and then treated with oxygen plasma for 10 minutes at 150 mTorr vacuum to activate negative surface charges on the glass. The multilayers of xGnP were prepared using a Microm DS 50 Slide Stainer purchased from Richard-Allan Scientific. The pretreated glass slides were immersed in the PDAC solution

for 20 minutes, followed by two 5-minutes rinses in DI water. Then the glass slides were immersed in graphite suspension for 30 min, followed by three 2-minutes rinses in DI water. The immersion time in xGnP is considered sufficient since longer time did not increase the surface coverage of xGnP. The sequence was repeated until the desired number of bilayers was formed. The substrates were dried naturally.

2.5. Characterization of xGnP and Polymer-Modified xGnP. Transmission electron microscopy (TEM) investigation was carried out with JEOL 100CX and JEOL 2200FS operating at a voltage of 100 keV and 200 keV for the morphology of xGnP. Specimens were prepared by ultrasonically dispersing the sample powders in acetone for 15 minutes, applying the powder suspension onto lacey carbon-coated Cu grids and drying them in air at ambient temperature. An X-ray photoelectron spectroscopy spectrum (XPS, Physical Electronics 5400 ESCA) was used to study the surface of xGnP and polymer modified xGnP. UV-vis absorption measurement was taken on a Perkin Elmer UV/Vis/NIR spectrometer (model Lamda 900). Thermogravimetric analysis (TGA) was performed using a TGA 2950 (TA instruments) from 25°C to 580°C at a heating rate of 10.0°C/min under an air flow. Approximately 10 mg of xGnP was used.

For Raman measurements, the xGnP thin films were prepared by filtering a certain amount of xGnP and polymer-coated xGnP on cellulose ester membrane with a pore size of 0.2 μm, and drying for a few days. The films were peeled off from the membrane before Raman measurement. The Raman characterization was carried out on a micro-Raman system with a laser wavelength of 532 nm and an intensity of 14.5 mW.

Both Zeta potential and particle size of xGnP were analyzed with Brookhaven Instruments ZetaPALS, which utilizes phase analysis light scattering (PALS) to determine the electrophoretic mobility of charged colloidal suspensions. The velocities of the charged particles were measured and the electrophoretic mobility was determined by dividing the measured velocity by the electric field strength. The zeta potential was determined from the electrophoretic mobility using the Smoluchowski equation. Before measurement, the polymer coated graphite nanoplatelets were suspended in DI water by sonication. The particle size was also analyzed with ZetaPALS incorporated with a 90Plus particle sizer. Since the principles of dynamic light scattering assume the particles to be spherical, only relative values of particle size were obtained. Each value of particle size is the average of ten measurements of the sample. For comparison, AcoustoSizer IIs (Colloidal Dynamics) was also used for measuring the particle size of xGnP. 120 mL of xGnP suspension with 1 wt% solid content was used.

2.6. Multilayers Characterizations. The morphology of single and multilayer films of xGnP on glass slides was characterized using scanning electron microscopy (SEM, JEOL 6300F). A layer of osmium was coated with a pure osmium coater (NEOC-AN, MEIWA SHOJI CO. LTD, JAPAN) for 20 s for enhanced conductivity before SEM measurements. The morphology of multilayer was also characterized using atomic force microscopy (AFM, a Nanoscope IV version from Veeco Instruments (Santa Barbara, CA)) in tapping mode. The surface resistance of xGnP multilayer was measured with a Camry Instruments Femtostat Station, and the transmittance was measured with Perkin Elmer Lambda 900 UV/Vis/NIR spectrometer.

3. Results and Discussions

Graphite has a layered structure with hybridized carbon atoms in an sp^2 configuration, and different layers are held together by van der Waals forces. Exfoliation of graphite is achieved by intercalation compounds which tend to exfoliate graphite upon heating due to the fast evaporation of intercalantes. A process was developed in our lab to produce exfoliated graphite nanoplatelets from a sulfuric acid-based intercalated graphite by microwave and sonication process, followed by a milling process to further reduce the particle size to approximately 1 μm. BET surface area analysis showed an area of approximately 100 m^2/g for the produced exfoliated graphite nanoplatelets [27]. Since a hypothetical monolayer graphite would exhibit a specific surface area close to 2700 m^2/g, and an interlayer spacing of 0.335 nm is assumed [28], the average thickness of graphite nanoplatelets was estimated to be 1–10 nm, which was further confirmed by TEM observation. As shown in Figure 1, the top view of xGnP shows clean surface of xGnP. It seems graphene sheets with different size are stacking together. Side view of xGnP clearly shows about 30 layers of atomic sheets stacking together, which counts to the thickness up to 10 nm.

To eliminate the need to search wide availability of surfactants and polyelectrolytes, the literature results of their ability for solublizing carbon nanotubes were adapted in this work. Therefore, a series of good surfactants and polyelectrolytes for carbon nanotubes were chosen to test for their ability to suspend and then self-assemble xGnP on the charged glass slides. They include sodium dodecylbenzene sulfonate (SDBS), sodium dodecyl sulfate (SDS), sulfated poly(styrene) (SPS), poly(acrylic acid) (PAA), and a conductive polymer blend: poly(3,4-ethylenedioxythiophene) poly(styrene sulfonate) (PEDT/SPS) was also used. In addition, a couple of positive polyelectrolytes, poly(diallyldimethylammonium chloride) (PDAC) and branched polyethyleimine (PEI) were also tested. Table 1 shows the summary of quick trial-and-error experiments. xGnP was dispersed in solution with the surfactants or polyelectrolytes and their stability was checked after 24 hours. The suspension with SDBS and SDS was relatively stable but self-assembly of xGnP resulted poor surface coverage of particles. Therefore, further study was not conducted on these surfactants. PDAC and PAA also showed poor dispersing ability. It was found that SPS and PEDT/SPS coated xGnP showed good stability in water. This is possibly due to the edge-to-face interactions between the graphitic surface and the aromatic rings of the polymer [29]. PEI is also a good suspending agent due to the hydrophobic interaction between PEI and uncharged graphitic surface [30].

Table 1: General performance of surfactants and polyelectrolytes on the solublization of xGnP and layer-by-layer deposition thereafter.

		Suspension After 24 hours	Layer-by-layer deposition
Surfactants	SDS	Partially settle down	Poor
	SDBS	Partially settle down	Poor
Polyelectrolytes	PDAC	Mostly settle down	Poor
	PEI	Stable	Good
	SPS	Stable	Very good
	PEDT/SPS	Stable	Good
	PAA	Mostly settle down	Poor

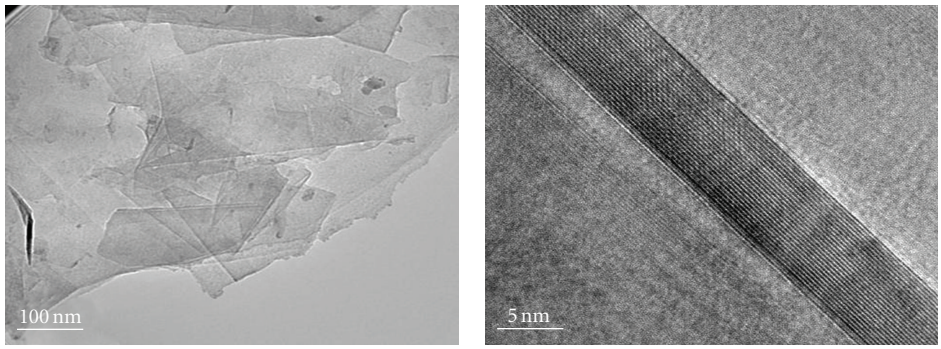

(a) (b)

Figure 1: Typical TEM images of xGnP: (a) top view and (b) side view.

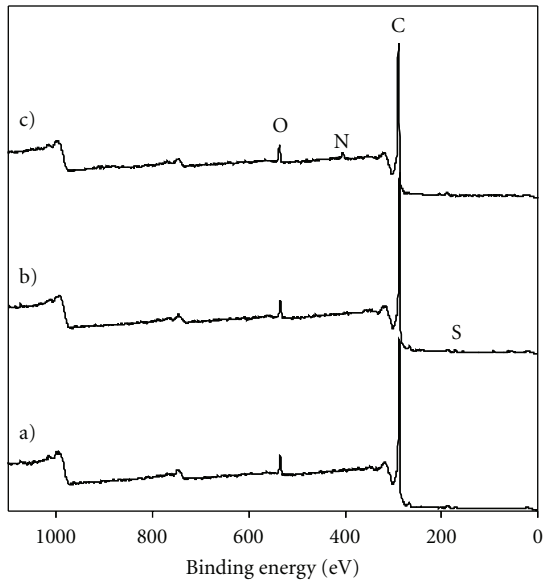

Figure 2: X-ray photoelectron spectroscopy spectra of xGnP before (a) and after SPS (b) and PEI (c) modification.

XPS was used to study the surface of xGnP before and after polymer coating. As shown in Figure 2, the surface of xGnP mainly contains C1s which shows peaks in the range of 280–290 eV. Small amount of oxygen is also shown which has an O1s peak at 540 eV. The oxygens mostly come from the edge group of the xGnP sheets such as carboxyl, hydroxyl, and carbonyl groups. There is also some Zr shown mainly due to the contamination of zirconium ball during the milling process. The SPS coated xGnP shows its characteristic peaks of S2p at 167.3 eV, corresponding to sulfone. PEI coated xGnP shows N1s peak at 401 eV. Therefore, XPS clearly shows the bonding of the polyelectrolyte to the graphite surface. Table 2 shows the detailed concentration of atoms for xGnP with and without polymer coatings. The amount of polymer coated on the surface is low. TGA was used to directly measure the amount of polymer coated on the xGnP. As shown in Figure 3, graphite is thermally stable in ambient air environments up to 500°C, and then it slightly decomposed at elevated temperature. The SPS coated xGnP shows a gradual loss due to the residue water, and a major degradation starts at approximately 360°C. Instead, both PEI and PDAC coated xGnP show the major degradation approximately at 200°C, which are much less thermally stable than SPS coated xGnP. It is clear that SPS has higher amount of coating on xGnP than PEI and PDAC, which is approximately 5 wt%. Stankovich et al. claimed that ~40 wt% of SPS is coated on graphite nanoplatelets when dispersing nanoplatelets with a thickness of ~4 nm [29]. Various concentrations of SPS and coating times were used to increase the coverage of polymer on xGnP, but no increase in SPS content on xGnP was observed.

The surface charges of polyelectrolytes coated xGnP and unmodified xGnP were characterized using a zeta potential analyzer. The zeta potential describes the nature of the electrostatic potential near the surface of a suspended particle. In general, agglomeration of particles could be avoided by electrostatic repulsion above certain surface potentials, which is approximately ±35 mV; and, the higher the absolute

Table 2: Atomic concentration of the surface of xGnP before and after PE modification.

	C1s	O1s	S2p	N1s	Zr3d
xGnP	92.38	6.38			0.25
SPS-xGnP	94.31	4.51	0.76		0.22
SPS-xGnP redispersed*	91.71	6.44	0.79		0.20
PEI-xGnP	91.84	4.73		3.19	0.25
PEI-xGnP redispersed*	90.69	5.79		3.24	0.28

* The xGnP was redispersed in DI water with mild sonication for 10–15 minutes, and then filtrated and dried before XPS measurement.

Table 3: Zeta potential of xGnP before and after the noncovalent attachment of polymers.

Materials	Zeta potential (mV)
xGnP	−32.33 ± 1.90
SPS-xGnP	−68.6 ± 0.75
PEDT/SPS-xGnP	−52.25 ± 1.49
PDAC-xGnP	49.39 ± 0.45
PEI-xGnP	48.56 ± 1.01

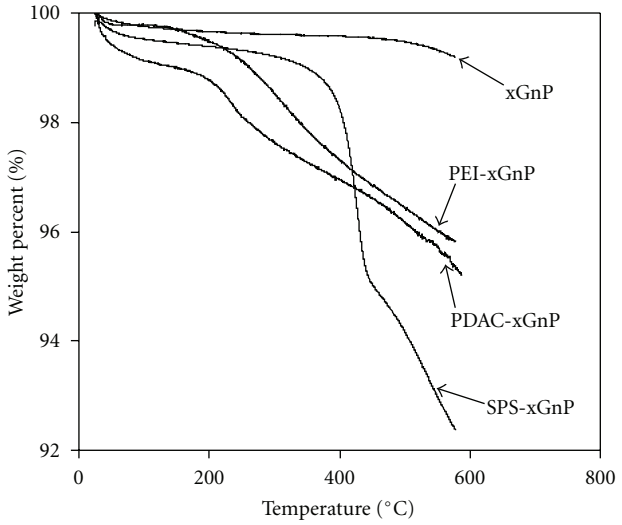

Figure 3: Thermogravimetric analysis of xGnP and polyelectrolytes modified xGnP.

value of the zeta potential, the more stable the particle suspension will be. In addition, the high surface charge of the modified graphite may count the strong van der Waals force between graphite nanoplatelets to prevent agglomeration during self-assembly. As shown in Table 3, the zeta potential for the unmodified xGnP was measured to be −32.33 mV, which is consistent with the literature value for the graphite particles [31]. The high absolute value of zeta potential for xGnP is possibly attributed to the naturally existing functional groups at the edges, such as carboxylic acid, hydroxyl, and so forth. The SPS and PEDT/SPS coated xGnP are kept negatively charged in aqueous solution, but the absolute value of zeta potential is increased to 68 mV for SPS coated xGnP, which confirms the significant adsorption of

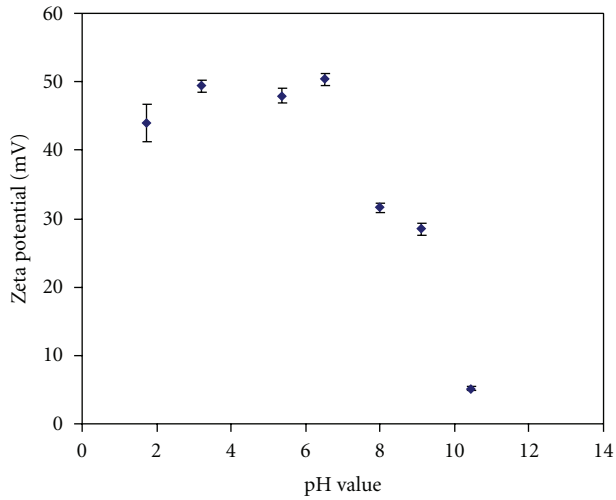

Figure 4: Zetal potential versus pH value for PEI coated xGnP.

SPS at the graphite surface. The zeta potential of PEDT/SPS coated xGnP is slightly lower (−52.25 mV), which is possibly due to the PEDT component in the conductive blend. For PDAC or PEI coated xGnP, the sign of the zeta potentials changed from negative to positive, and the magnitude of the positive zeta potential increased. By a simple comparison of the absolute values of zeta potential, the SPS coated xGnP suspension shows better stability than xGnP coated with other polyelectrolytes. The zeta potentials of PEI coated nanoplatelets varied with the pH value of the solution, thus the suspension stability varied. As shown in Figure 4, the zeta potential of PEI coated xGnP keeps relatively constant at a value of 48 mV when the pH is below 7, because the PEI molecules are mostly protonated which results strong repulsive force between the charged segments ($\mathbf{pK_a}$ of PEI is greater than 8.0). When the pH value is above 7, the zeta potential significantly decreases with increasing pH value due to uncharged PEI molecules. At the pH value of 10.5, the PEI coated xGnP has no net charge. The stability of xGnP suspension is fully correlated with the zeta potential of particles. Figure 5 shows the PEI coated xGnP dispersed in DI water with adjustment to the varied pH values after sitting for 24 hours. The suspension was relatively stable when the pH value is close to 7 or below. However, when the pH value is above 10, the graphite nanoplatelets completely settle out of solution.

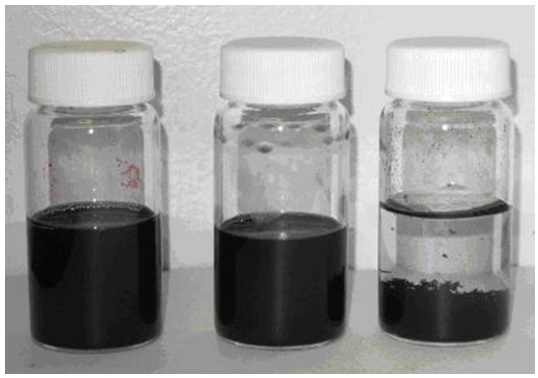

(a) (b) (c)

Figure 5: The stability of PEI coated xGnP at different solution pH values. (a) 5.33, (b) 7.16, and (c) 10.46.

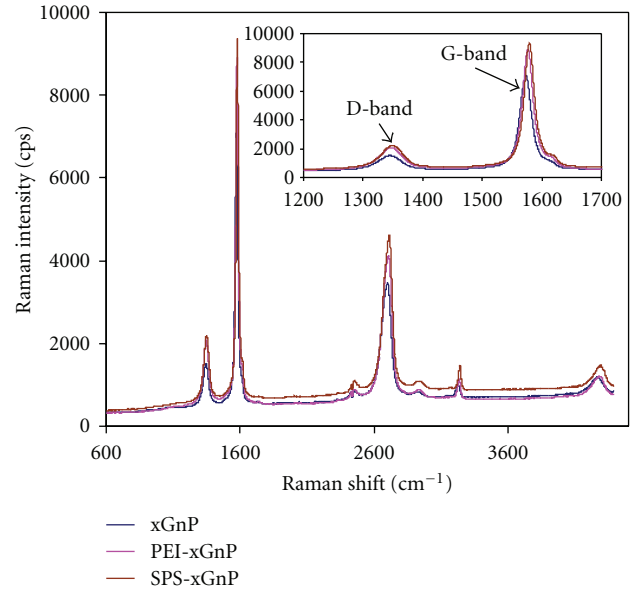

Figure 6: Raman spectra of xGnP before and after modification with polyelectrolytes (inset: enlargement of D-band and G-band).

The stability of xGnP suspension was further quantified by measuring the concentration difference of suspension and corresponding particles size before and after sitting for 48 hours. As discussed before, when the zeta potential of particle is above 35 mV, the repulsive force between particles can overcome the attractive van der Waals force, and the agglomeration of particles can be prevented. For graphite nanoplatelets, zeta potential may not fully characterize the stability of suspension, because the high zeta potential could mostly be attributed to the edge effect, and the large hydrophobic basal plane can be attracted by each other. In addition, the surface charge is limited and may not fully account for the particle size. The comparison of the xGnP concentration before and after allowing the suspension to sit for 48 hours is a good indication of the stability. For both SPS and PEI coated xGnP, approximately 45% of xGnP still remain in the solution and the other settles down. The top layer suspension is very stable, no further sedimentation occurs after a week. The analysis of average particle size by dynamic light scattering gives further insight on this. The average particle size of xGnP was measured to be 911.3 ± 47.8 nm. Although the principles of dynamic light scattering assume the particles measured to be spherical, the measured particle size of xGnP is close to the one observed with microscopic technique. In addition, a different technique was used to measure the particle size using AcoustoSizer IIs (Colloidal Dynamics), which uses electroacoustic signal to determine the dynamic mobility of the particles in a colloidal suspension. It gave a similar particle size for xGnP (data not shown). The particle size distribution shows that xGnP has approximately 30% which has a particle size above 1 μm (data not shown). In the top solution after sitting for 48 hours, the average particle size was measured to be 442.1 ± 13.1 nm, and 98% of particle is below 634.9 nm, meaning that most big particles are eliminated. We have also looked at the particle size of xGnP for a highly stable supernatant after centrifuge, which shows a value of 200.9 ± 6.2 nm. Therefore, the stability of xGnP suspension is determined by both surface charge and particle size.

The bonding strength of the polymer chains to the surface of xGnP can be measured by Raman spectrometry, because the presence of the polymer can affect the movement of carbon atoms [32]. The Raman spectra of xGnP and polymer coated xGnP are shown in Figure 6. The xGnP shows typical bands of graphite in the presence of disorder [33, 34]. The band at 1575 cm^{-1} is so called G-band resulting from the doubly degenerate zone center E_{2g} mode [33]. The peak in the 1300–1400 cm^{-1} region is the disorder peak known as the D-band, which is attributed to scattering from sp^2 carbons containing defects. The peak between 2700 and 2800 cm^{-1} is D* mode, which is an overtone of the D band [33]. By inspecting the spectra before and after polymer coating, it was found that both the intensity and spectral position of D band and G band have changed. In the presence of both PEI and SPS, the D band is slightly shifted to higher wave numbers, approximately 2–4 cm^{-1}, and the position of the G band is shifted 3–6 cm^{-1} higher. The intensity and sharpness of the D band and G band increase; in addition, the ratio of the intensify of D band to that of the G-band slightly increases from 0.21 for xGnP to 0.23 for both PEI and SPS coated xGnP. Although the change in Raman spectra is not significant, it clearly indicates a typical noncovalent modification of the graphene sheet [32]. The upshift of the D and G band is possibly due to the hydrophobic and van der Waals forces between the polymer and the graphite sheet, which increase the energy necessary for vibrations to occur. And the slight increase in disorder structure after polymer coating is possibly due to the remaining carbon atoms from the polymer coating [32] and the field disturbance and physical strain in the graphene sheet caused by the interactions with the polymers. It was also noticed that the peak shift and intensity increase in Raman spectrum for SPS coated xGnP is more significant

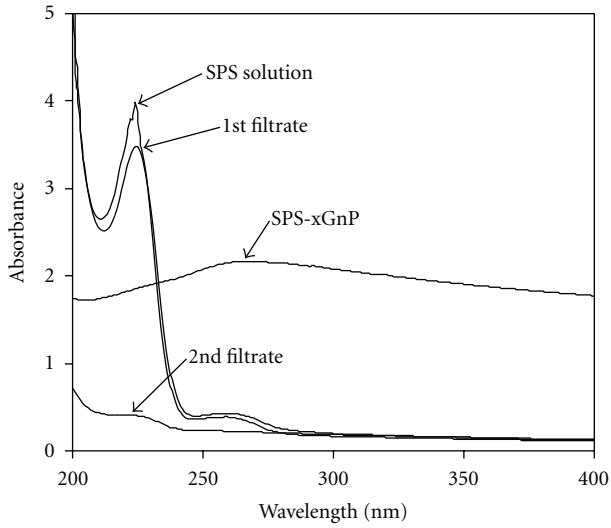

Figure 7: The UV-Vis spectra of SPS, SPS-xGnP and the filtrates obtained during the filtration process.

than those for PEI coated xGnP, which implies that SPS has a stronger interaction force with the graphene surface than PEI. This is possibly due to the molecular similarity of SPS to the graphene structure. At a high solution pH, where PEI is unprotonated, hydrophobic or Van der Waals forces could be the main driving force. During adsorption, PEI chains can be arranged on the hydrophobic basal plane in an extended conformation [35]. Although single molecules were found on the graphite surface, it is more possible for agglomerations form due to the lack of repulsive force between the molecules [30].

Most work reported so far regarding the self-assembly of carbon nanotubes using polymer noncovalent bonding involving the simple dispersion of carbon nanotubes in polyelectrolyte solution by sonication with no further purification [36, 37]. In this work, we found that the excess polyelectrolyte in the xGnP suspension plays a significant role in the self-assembly process. LbL assembly typically involves diffusion and adsorption processes, in which size matters. With the excess free polyelectrolytes, the surface coverage of xGnP on the glass slide was low. Therefore, it is necessary to remove the excess PEs that was not attached to xGnP. The stability of the adsorbed PE chains on graphite during filtration, the subsequent rinsing with water and redispersion utilizing sonication were examined with UV-vis spectroscopy and XPS. As shown in Figure 7, the spectrum of SPS shows a typical absorption peak at 222 nm, and the peak height of 1st filtrate after coating with xGnP decreased, indicating some SPS is deposited on xGnP. The SPS coated xGnP was rinsed with DI water for three times, and then redispersed in DI water by mild sonication. The second filtrate shows a very small peak at 222 nm, which could result from the incomplete wash or dissociation of polymer due to sonication. Surprisingly, there is no SPS peak showing in the spectrum of SPS-xGnP, which is possible due to the extremely low concentration of xGnP in the sample. XPS was further used to confirm that SPS remains on the xGnP after the washing and sonication process. As shown in Table 2, the S2p atom content for SPS-xGnP after redispersing with sonication is close to the one before, indicating there is no loss of SPS from xGnP during washing and redispersion. The same result is observed for PEI-xGnP, indicated by the N1s content.

LbL self-assembly is a versatile technique to produce robust films with precise control on the film thickness and properties. With their one dimensional nanometer size, electrostatically charged PE coated surface, and their ability to form a stable colloidal dispersion, the PE modified graphite nanoplatelets are ideal candidates for multilayer self-assembly. SPS coated xGnP combined with PDAC was used to demonstrate the LbL assembly process. Optical microscopy images (not shown) of a single bilayer of PDAC/SPS coated xGnP show that the surface coverage of xGnP is low, possibly due to the large particle size, limiting the diffusion and repulsive electrostatic forces. With further multilayer growth, more graphite particles fill into the gaps or stack on the existing particles. At 10 bilayers, the surface became visibly black. Figures 8 and 9 show the SEM images of 4 and 10 xGnP bilayers, respectively. At low magnification, Figure 8(a) shows most agglomerates of graphite particle, and they seem isolated. At high magnification (Figures 8(b) and 8(c)), it is clear that these graphite agglomerates are bridged with graphene platelets with nanometer thicknesses. The edges of agglomerates and nanoplatelets are curled or folded which disrupts the packing of xGnP. Figure 9 shows a relatively dense packing of xGnP at 10 bilayers, but with the varying size and shape of the platelets, the surface of multilayer film is very rough.

The AFM image in Figure 10 shows a clear layered structure of graphene sheets, and all the nanoplatelets are stacking together and relatively close to one another. The roughness analysis of the AFM image shows a very rough surface of the multilayer film, and the section analysis shows that the thickness of 10 bilayers is in the range of 400 to 800 nm, which is much thicker than the theoretical value of 10 bilayers. xGnP/polyelectrolytes multilayers can also be fabricated with PEI-xGnP and SPS as the counter ion. It was found the surface coverage of xGnP was much lower than SPS-xGnP/PDAC multilayers (images not shown), which is possible due to the lower surface charge of PEI-xGnP, limiting their ability to be adsorbed on the surface.

One possible application of xGnP thin film is as an inexpensive conductive coating. Thus, the resistance and transmittance of xGnP multilayers were measured. Figure 11 shows the resistance of the glass slides coated with PDAC/SPS coated xGnP multilayer. The log(resistance) at 1 Hz for the glass slide is 11.13, which is nonconductive. Glass slides coated with PDAC/SPS coated xGnP are non conductive until 4 bilayers, indicating that a percolation threshold is reached. This result is consistent with the OM and SEM observation. The resistance of the films continually decreases with more multilayers deposited on the surface. The log(resistance) at 1 Hz reaches 4.85 for 10 PDAC/SPS-xGnP bilayer film. Recently, transparent conductive carbon

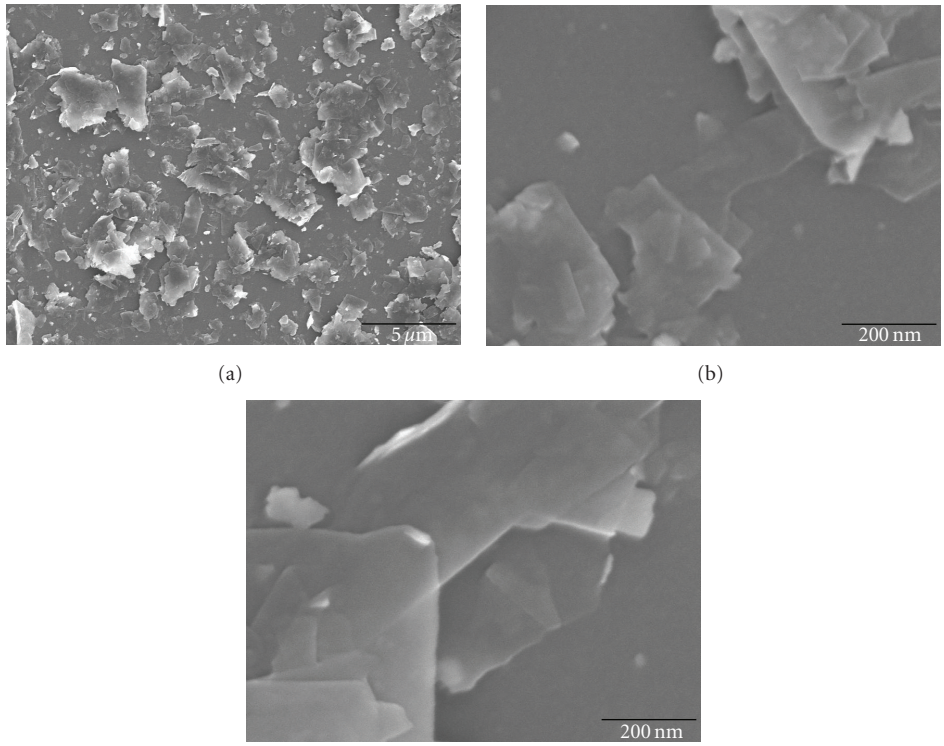

(a) (b)

(c)

Figure 8: SEM images of 4 bilayers of PDAC/SPS-xGnP (a) low magnification (scale bar: 5 μm), (b) and (c) high magnification (scale bar: 200 nm).

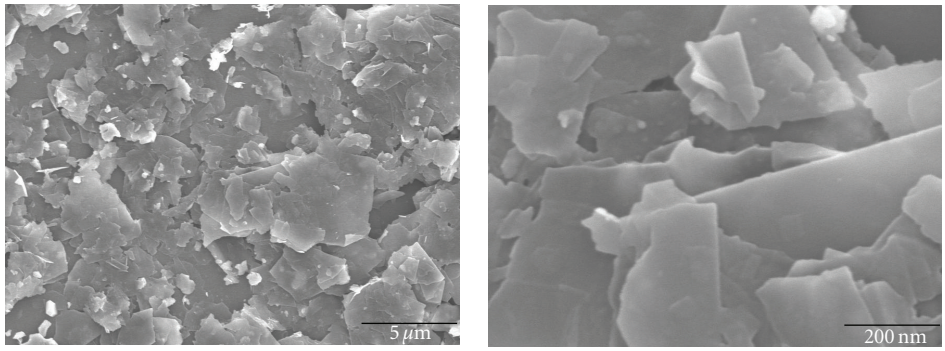

(a) (b)

Figure 9: SEM images of 10 bilayers of PDAC/SPS-xGnP (a) low magnification (scale bar: 5 μm), and (b) high magnification (scale bar: 200 nm).

nanotube films have attracted much attention due to their possible application in modern technology, such as video displays, solar cells, lasers, optical communication devices, and solid state lighting [36, 38–40]. We are pursuing the replacement of carbon nanotubes with inexpensive xGnP in these applications. Figure 12 shows the transmittance of xGnP multilayers which were measured by the UV-vis spectrometer at 500 nm wavelength. Unfortunately, the increase in the conductivity of the film is accompanied with a dramatic decrease in the transmittance of the glass slides. The transmittance of the glass slide coated on both sides is 11.89% when the surface is conductive (4 bilayers), and the transmittance decreases to 2.74% at 10 bilayers. The loss of transmittance suffers from the way that graphite deposited on the surface; curled and turned-in edges of the sheets, and the agglomeration of nanoplatelets cause the high thickness of the layers. Further work is being conducted to increase the conductivity and transmittance of xGnP containing films using different preparation techniques, such as Langmuir-Blodgett methods and filtration methods. Patterned conductive multilayered xGnP composite film was also developed for applications in electronic devices [41].

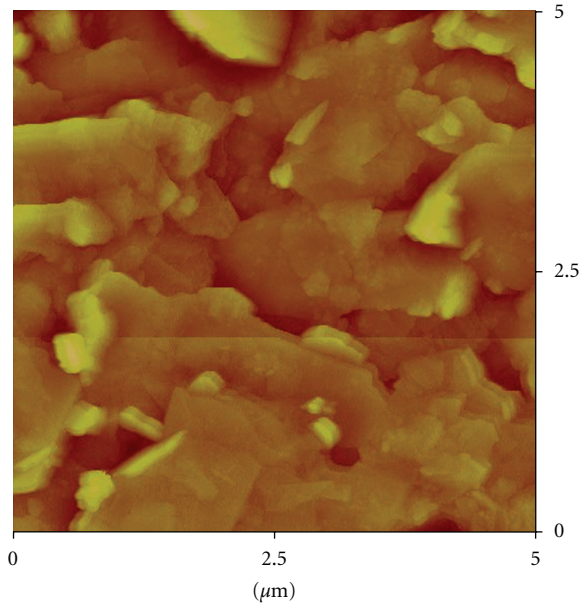

Figure 10: Height AFM image of 10 bilayers of PDAC/SPS-xGnP (color scale: black to bright yellow, 1200 nm).

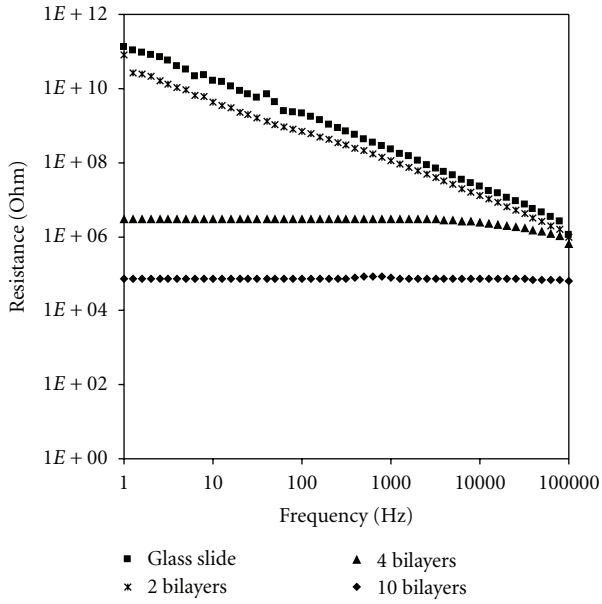

Figure 11: Resistance measurement of glass slide and xGnP multilayers.

4. Conclusions

In summary, we have achieved the stable aqueous suspension of graphite nanoplatelets, which are an inexpensive nanomaterial, by the noncovalent functionalization with polyelectrolytes. A variety of surfactants and polyelectrolytes have been compared for their ability to suspend graphite nanoplatelets. This noncovalent method is better for preserving the mechanical and electrical properties of graphite platelets compared to the traditional oxidation methods.

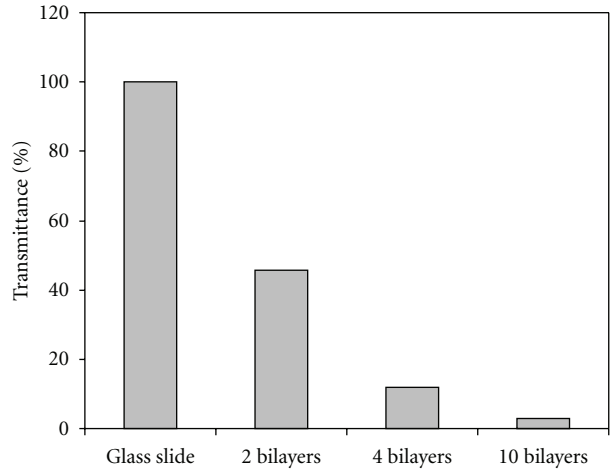

Figure 12: Transmittance of glass slides coated on both sides with various bilayers of PDAC/SPS-xGnP.

This robust method opens up the possibility of using these inexpensive nanomaterials in many applications, including electrochemical devices, and provides the way to processing techniques such as LbL deposition. We have demonstrated that conductive coating can be achieved by LbL assembly of polyelectrolyte-functionalized graphite nanoplatelets. Multilayer PDAC/SPS-xGnP film deposition reached the percolation threshold in only 4 cycles, resulting in a conductive thin film. The resistance of the film was lowered with more deposition cycles. However, the average roughness of these multilayer films was high, and the thickness of films was higher than theoretically estimated. This occurred because the edges of graphite nanoplatelets fold which affects the dense packing of the nanoplatelets; in addition, the nanoplatelets tend to overlap with each other. This also attributes to the low surface resistance and transmittance of xGnP films. Further work is on going to increase the film conductivity and transmittance using different processing methods, such as Langmuir-Blodgett and filtration.

Acknowledgment

The funding from the National Science Foundation (CBET-0609164, CMMI-0832730), the University Research Corridor, the Michigan Economic Development Corporation, and the MSU Foundation to support this research is greatly appreciated.

References

[1] P. T. Hammond, "Form and function in multilayer assembly: new applications at the nanoscale," *Advanced Materials*, vol. 16, no. 15, pp. 1271–1293, 2004.

[2] K. Ishibashi, S. Moriyama, D. Tsuya, T. Fuse, and M. Suzuki, "Quantum-dot nanodevices with carbon nanotubes," *Journal of Vacuum Science and Technology A*, vol. 24, no. 4, pp. 1349–1355, 2006.

[3] M. Lee, J. Im, B. Y. Lee et al., "Linker-free directed assembly of high-performance integrated devices based on nanotubes and

nanowires," *Nature Nanotechnology*, vol. 1, no. 1, pp. 66–71, 2006.

[4] K. Lee, J. Zhang, H. Wang, and D. P. Wilkinson, "Progress in the synthesis of carbon nanotube- and nanofiber-supported Pt electrocatalysts for PEM fuel cell catalysis," *Journal of Applied Electrochemistry*, vol. 36, no. 5, pp. 507–522, 2006.

[5] C. Lynam, S. E. Moulton, and G. G. Wallace, "Carbon-nanotube biofibers," *Advanced Materials*, vol. 19, no. 9, pp. 1244–1248, 2007.

[6] Y. Lin, W. Yantasee, and J. Wang, "Carbon nanotubes (CNTs) for the development of electrochemical biosensors," *Frontiers in Bioscience*, vol. 10, pp. 492–505, 2005.

[7] C. M. Welch and R. G. Compton, "The use of nanoparticles in electroanalysis: a review," *Analytical and Bioanalytical Chemistry*, vol. 384, no. 3, pp. 601–619, 2006.

[8] A. C. Ferrari, J. C. Meyer, V. Scardaci et al., "Raman spectrum of graphene and graphene layers," *Physical Review Letters*, vol. 97, no. 18, Article ID 187401, 4 pages, 2006.

[9] A. K. Geim and K. S. Novoselov, "The rise of graphene," *Nature Materials*, vol. 6, no. 3, pp. 183–191, 2007.

[10] X. Li, W. Cai, J. An et al., "Large-area synthesis of high-quality and uniform graphene films on copper foils," *Science*, vol. 324, no. 5932, pp. 1312–1314, 2009.

[11] D. D. L. Chung, "Exfoliation of graphite," *Journal of Materials Science*, vol. 22, no. 12, pp. 4190–4198, 1987.

[12] W.-X. Chen, J. Y. Lee, and Z. Liu, "Preparation of Pt and PtRu nanoparticles supported on carbon nanotubes by microwave-assisted heating polyol process," *Materials Letters*, vol. 58, no. 25, pp. 3166–3169, 2004.

[13] H. Fukushima, "Graphite nanoreinforcements in polymer nanocomposites," in *PhD Dissertation in Department of Chemical Engineering and Materials Science*, Michigan State University, East Lansing, Mich, USA, 2003.

[14] S. Stankovich, D. A. Dikin, G. H. B. Dommett et al., "Graphene-based composite materials," *Nature*, vol. 442, no. 7100, pp. 282–286, 2006.

[15] I.-H. Do, "Metal decoration of exfoliated graphite nanoplatelets (xGnP) for fuel cell applications," in *PhD Dissertation in Department of Chemical Engineering and Materials Science*, Michigan State University, East Lansing, Mich, USA, 2006.

[16] J. Lu, I. Do, L. T. Drzal, R. M. Worden, and I. Lee, "Nanometal-decorated exfoliated graphite nanoplatelet based glucose biosensors with high sensitivity and fast response," *ACS Nano*, vol. 2, no. 9, pp. 1825–1832, 2008.

[17] J. Lu, L. T. Drzal, R. M. Worden, and I. Lee, "Simple fabrication of a highly sensitive glucose biosensor using enzymes immobilized in exfoliated graphite nanoplatelets Nafion membrane," *Chemistry of Materials*, vol. 19, no. 25, pp. 6240–6246, 2007.

[18] W. Zhao, C. Song, and P. E. Pehrsson, "Water-soluble and optically pH-sensitive single-walled carbon nanotubes from surface modification," *Journal of the American Chemical Society*, vol. 124, no. 42, pp. 12418–12419, 2002.

[19] E. T. Mickelson, I. W. Chiang, J. L. Zimmerman et al., "Solvation of fluorinated single-wall carbon nanotubes in alcohol solvents," *Journal of Physical Chemistry B*, vol. 103, no. 21, pp. 4318–4322, 1999.

[20] V. C. Moore, M. S. Strano, E. H. Haroz et al., "Individually suspended single-walled carbon nanotubes in various surfactants," *Nano Letters*, vol. 3, no. 10, pp. 1379–1382, 2003.

[21] G. Decher, "Fuzzy nanoassemblies: toward layered polymeric multicomposites," *Science*, vol. 277, no. 5330, pp. 1232–1237, 1997.

[22] X. Wang, H.-X. Huang, A.-R. Liu et al., "Layer-by-layer assembly of single-walled carbon nanotube-poly(viologen) derivative multilayers and their electrochemical properties," *Carbon*, vol. 44, no. 11, pp. 2115–2121, 2006.

[23] T. Cassagneau and J. H. Fendler, "High density rechargeable lithium-ion batteries self-assembled from graphite oxide nanoplatelets and polyelectrolytes," *Advanced Materials*, vol. 10, no. 11, pp. 877–881, 1998.

[24] T. Cassagneau, F. Guérin, and J. H. Fendler, "Preparation and characterization of ultrathin films layer-by-layer self-assembled from graphite oxide nanoplatelets and polymers," *Langmuir*, vol. 16, no. 18, pp. 7318–7324, 2000.

[25] N. A. Kotov, I. Dékány, and J. H. Fendler, "Ultrathin graphite oxide-polyelectrolyte composites prepared by self-assembly: transition between conductive and non-conductive states," *Advanced Materials*, vol. 8, no. 8, pp. 637–641, 1996.

[26] N. I. Kovtyukhova, P. J. Ollivier, B. R. Martin, et al., "Layer-by-layer assembly of ultrathin composite films from micron-sized graphite oxide sheets and polycations," *Chemistry of Materials*, vol. 11, no. 3, pp. 771–778, 1999.

[27] L. T. Drzal and H. Fukushima, "Expanded graphite and products produced therefrom," 2004, US Patent application 20040127621.

[28] W. N. Reynolds, *Physical Properties of Graphite*, Elsevier, Amsterdam, The Netherlands, 1968.

[29] S. Stankovich, R. D. Piner, X. Chen, N. Wu, S. T. Nguyen, and R. S. Ruoff, "Stable aqueous dispersions of graphitic nanoplatelets via the reduction of exfoliated graphite oxide in the presence of poly(sodium 4-styrenesulfonate)," *Journal of Materials Chemistry*, vol. 16, no. 2, pp. 155–158, 2006.

[30] M. Schneider, M. Brinkmann, and H. Möhwald, "Adsorption of polyethylenimine on graphite: an atomic force microscopy study," *Macromolecules*, vol. 36, no. 25, pp. 9510–9518, 2003.

[31] V. K. Paruchuri, A. V. Nguyen, and J. D. Miller, "Zeta-potentials of self-assembled surface micelles of ionic surfactants adsorbed at hydrophobic graphite surfaces," *Colloids and Surfaces A*, vol. 250, no. 1–3, pp. 519–526, 2004.

[32] V. A. Sinani, M. K. Gheith, A. A. Yaroslavov et al., "Aqueous dispersions of single-wall and multiwall carbon nanotubes with designed amphiphilic polycations," *Journal of the American Chemical Society*, vol. 127, no. 10, pp. 3463–3472, 2005.

[33] S. Reich and C. Thomsen, "Raman spectroscopy of graphite," *Philosophical Transactions of the Royal Society A*, vol. 362, no. 1824, pp. 2271–2288, 2004.

[34] F. Tuinstra and J. L. Koenig, "Raman spectrum of graphite," *Journal of Chemical Physics*, vol. 53, no. 3, pp. 1126–1130, 1970.

[35] J. Park and P. T. Hammond, "Polyelectrolyte multilayer formation on neutral hydrophobic surfaces," *Macromolecules*, vol. 38, no. 25, pp. 10542–10550, 2005.

[36] M. Palumbo, K. U. Lee, B. T. Ahn et al., "Electrical investigations of layer-by-layer films of carbon nanotubes," *Journal of Physics D*, vol. 39, no. 14, pp. 3077–3085, 2006.

[37] H. Paloniemi, M. Lukkarinen, T. Ääritalo et al., "Layer-by-layer electrostatic self-assembly of single-wall carbon nanotube polyelectrolytes," *Langmuir*, vol. 22, no. 1, pp. 74–83, 2006.

[38] T. M. Barnes, X. Wu, J. Zhou et al., "Single-wall carbon nanotube networks as a transparent back contact in CdTe solar cells," *Applied Physics Letters*, vol. 90, no. 24, Article ID 243503, 3 pages, 2007.

[39] A. Schindler, J. Brill, N. Fruehauf, J. P. Novak, and Z. Yan IV, "Solution-deposited carbon nanotube layers for flexible display applications," *Physica E: Low-Dimensional Systems and Nanostructures*, vol. 37, no. 1-2, pp. 119–123, 2007.

[40] Z. Wu, Z. Chen, X. Du et al., "Transparent, conductive carbon nanotube films," *Science*, vol. 305, no. 5688, pp. 1273–1276, 2004.

[41] T. R. Hendricks, J. Lu, L. T. Drzal, and I. Lee, "Intact pattern transfer of conductive exfoliated graphite nanoplatelet composite films to polyelectrolyte multilayer platforms," *Advanced Materials*, vol. 20, no. 10, pp. 2008–2012, 2008.